Communication

A Self-Ordered, Crystalline Glass, Mesoporous Nanocomposite with High Proton Conductivity of 2 × 10 S cm at Intermediate Temperature

Masanori Yamada, Donglin Li, Itaru Honma, and Haoshen Zhou

J. Am. Chem. Soc., **2005**, 127 (38), 13092-13093• DOI: 10.1021/ja052914x • Publication Date (Web): 02 September 2005

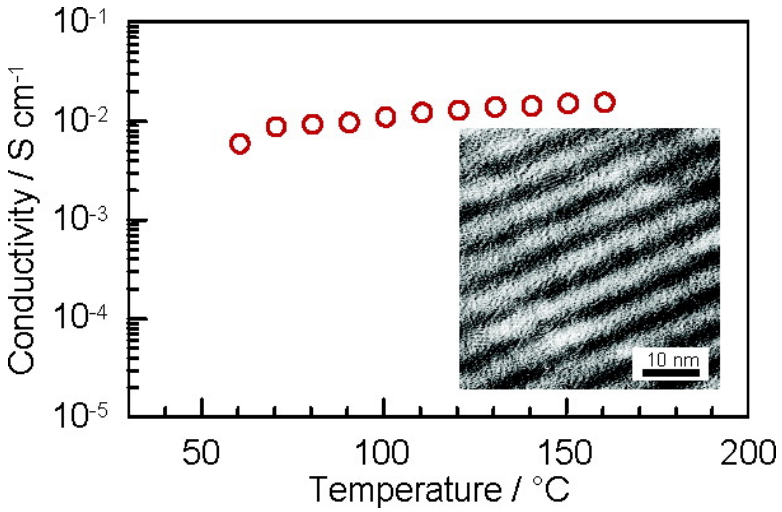

More About This Article

Additional resources and features associated with this article are available within the HTML version:

- Supporting Information
- Links to the 7 articles that cite this article, as of the time of this article download
- Access to high resolution figures
- Links to articles and content related to this article
- Copyright permission to reproduce figures and/or text from this article

View the Full Text HTML

J|A|C|S
COMMUNICATIONS

Published on Web 09/02/2005

A Self-Ordered, Crystalline Glass, Mesoporous Nanocomposite with High Proton Conductivity of 2×10^{-2} S cm^{-1} at Intermediate Temperature

Masanori Yamada, Donglin Li, Itaru Honma, and Haoshen Zhou*

Energy Technology Research Institute, National Institute of Advanced Industrial Science and Technology (AIST), Umezono 1-1-1, Tsukuba, Ibaraki 305-8568, Japan

Received May 4, 2005; E-mail: hs.zhou@aist.go.jp

Fuel cells are an extremely attractive energy conversion system for use in many industrial applications, including electric vehicles (EV) and on-site power plant, due to their inherently higher efficiency and lower emission when compared to that of internal combustion engines. Especially, the operation of proton exchange membrane fuel cell (PEMFC) at intermediate temperature (130−200 °C) has been considered to provide many advantages, such as improved CO tolerance of the Pt electrode, the reduction of the amount of Pt electrode materials, the higher energy efficiency, heat management, and cogenerations.[1,2] However, customary hydrated perfluorosulfonic membranes, such as Nafion, are unstable at intermediate temperature, and proton conductivity decreases by the evaporation of water from the membrane and degradations of the molecular structure by irreversible reactions.[3] Therefore, a proton conductor with high proton conductivity at intermediate temperatures has attracted much interest recently for solving problems in the current technologies.[1,2]

Mesoporous inorganic materials have a pore size range of 2−50 nm and have several properties that may be beneficial for their use as possible solid-state electrolyte alternatives.[4−6] They include high specific surface area, open channels of large dimension, and open framework with an ordered or disordered interconnected internal structure, and chemical, structural, and mechanical variability that allows for significant optimization of electrochemical performance.[6,7] Therefore, mesoporous materials as a proton conducting electrolyte for fuel cells have been reported.[8] These mesoporous materials show the proton conductivity of 10^{-3}−10^{-2} S cm^{-1} at 25 °C under fully saturated humidification conditions (100% RH).[8] However, at the intermediate temperature region, proton conductivity decreases by the evaporation of water because the origin of proton conduction in mesoporous material is based on the physisorbed water in the pore. Therefore, the mesoporous material with the high proton conductivity at the intermediate temperature region under 100% RH conditions has been hardly reported as far as we know.

Recently, we synthesized a $TiO_2-P_2O_5$ self-ordered, crystalline glass, mesoporous nanocomposite (CGMN) with a high thermal stability.[9] This $TiO_2-P_2O_5$ CGMN has a high water-holding capacity by the chemisorption because the P_2O_5 constructs the P−OH group under high humidity conditions.[10] Furthermore, $TiO_2-P_2O_5$ CGMN with crystal glass configuration is the thermostable material. Herein, we propose the utilization of $TiO_2-P_2O_5$ CGMN as a new intermediate temperature solid-state electrolyte for fuel cells. As a result, $TiO_2-P_2O_5$ CGMN indicates the high proton conductivity of 10^{-2} S cm^{-1} at 160 °C under 100% RH conditions. Additionally, these conductivities were stable at intermediate temperature conditions.

The $TiO_2-P_2O_5$ CGMN was synthesized by the previously reported procedure.[9] The Brunauer−Emmett−Teller (BET) surface area of $TiO_2-P_2O_5$ CGMN was about 200 m^2 g^{-1}. Figure 1 shows the TEM images of $TiO_2-P_2O_5$ CGMN. The $TiO_2-P_2O_5$ CGMN indicated a uniform pore size with a diameter of 4 nm and a framework of 5 nm widths in the TEM images. The details of the TEM image are given in ref 9. These uniform structures and distances were also confirmed by the X-ray diffraction patterns (XRD).[9]

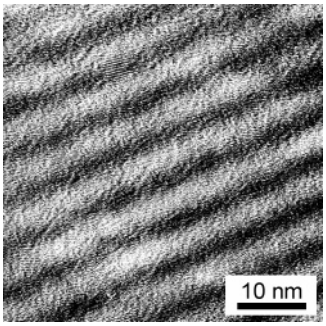

Figure 1. TEM images of $TiO_2-P_2O_5$ CGMN.

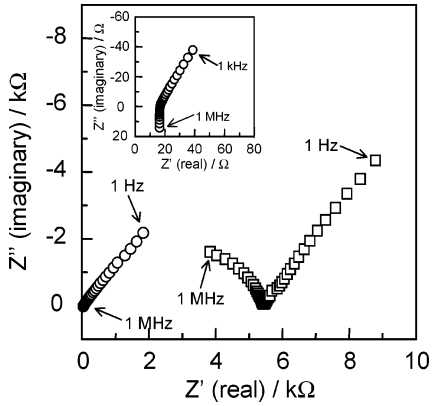

Figure 2. Typical impedance response (Cole−Cole plots) of (○) $TiO_2-P_2O_5$ CGMN and (□) mesoporous silica at 160 °C under 100% RH conditions. Frequency range is from 1 Hz to 1 MHz. The insert indicated the high-frequency range (1 kHz to 1 MHz) of $TiO_2-P_2O_5$ CGMN.

The powder sample of $TiO_2-P_2O_5$ CGMN was compacted into pellets and sandwiched between two gold electrodes. Additionally, we also used mesoporous silica, which can hold physisorbed water, as a comparative material. The proton conductivity measurements were demonstrated by the a.c. impedance method over the frequency range from 1 Hz to 1 MHz under 100% RH. In contrast, these samples did not indicate the electronic conductivity at the DC condition. Additionally, the diffusible ions, other than protons, have not existed in materials. Therefore, the measured impedance response indicates the proton conduction. Figure 2 shows the typical impedance response (Cole−Cole plots) of (○) $TiO_2-P_2O_5$ CGMN and (□) mesoporous silica at 160 °C under 100% RH conditions. The insert indicated the high-frequency range (1 kHz to 1 MHz)

10.1021/ja052914x CCC: $30.25

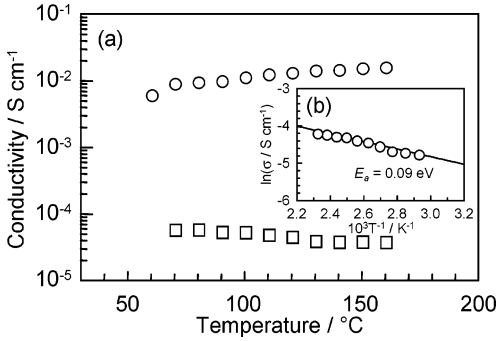

Figure 3. (a) Proton conductivity of (○) $TiO_2-P_2O_5$ CGMN and (□) mesoporous silica in the temperatures range from RT to 160 °C under 100% RH conditions. (b) Arrhenius plots of the conductivity of $TiO_2-P_2O_5$ CGMN. Solid line is the result of the least-squares fitting. Activation energy (E_a) of the proton transport under 100% RH conditions was estimated from the slope.

of $TiO_2-P_2O_5$ CGMN. A typical Cole−Cole plot of $TiO_2-P_2O_5$ CGMN showed a feature similar to that of a highly proton conducting membrane, such as Nafion,[3] the organic−inorganic hybrid membrane mixed with heteropolyacids[11] and biomolecules composite materials.[12] The resistances of CGMN were obtained from the extrapolation to the real axis.

Figure 3a shows the proton conductivity of (○) $TiO_2-P_2O_5$ CGMN and (□) mesoporous silica in the temperature range from RT to 160 °C under 100% RH conditions. The proton conductivities of $TiO_2-P_2O_5$ CGMN lightly increased with the cell temperature and reached a maximum conductivity at 160 °C. Surprisingly, the $TiO_2-P_2O_5$ CGMN indicated the high proton conductivity of 1.6 $\times$ 10^{-2} S cm^{-1} at 160 °C under 100% RH conditions. These proton conductivities are as high a value as the inorganic proton conductor at intermediate temperature under 100% RH conditions. In contrast, mesoporous silica did not show the high proton conductivity; additionally, this conductivity slightly decreased with the increase of cell temperature because the hydrate water in the pore structure evaporates. So, to discuss the proton-transfer mechanism in CGMN material, we determined the activation energy (E_a) of proton conduction in mesoporous material. Figure 3b shows the Arrhenius plots of proton conductivity of $TiO_2-P_2O_5$ CGMN. Solid lines in Figure 3b are the results of the least-squares fitting. The E_a values of proton conduction were estimated from the slope. The E_a of $TiO_2-P_2O_5$ CGMN was 0.09 eV. In contrast, mesoporous silica could not calculate the E_a since the proton conductivity decreased with the increase of cell temperature. This E_a is lower than that of anhydrous proton conductor (E_a = >0.2 eV) based on a proton hopping mechanism.[12−14] In fact, the proton conductivity of $TiO_2-P_2O_5$ CGMN was sensitive for the humidity, and this material could not give measurable proton conductivity (on the order of 10^{-7} S cm^{-1}) at 160 °C under anhydrous conditions (see Figure S1 in Supporting Information). These results suggest that the conduction behavior is controlled by the H_3O^+- or $H_5O_2^+$-mediated charge transport.[13,14] We have considered as follows: the proton transfer in $TiO_2-P_2O_5$ CGMN with a high surface area is based on water behavior that chemisorbed on the pore wall because the P_2O_5 constructs the P−OH group under high humidity conditions.[10] Therefore, the activation energy of 0.09 eV is related to the energy necessary for the dissociation of a proton from the hydroxyl group.

Inorganic proton conductors with the high proton conductivity of 1 $\times$ 10^{-2} S cm^{-1}, such as heteropolyacids (e.g., $H_3PW_{12}O_{40}\cdot 29H_2O$ and $H_6GeW_{10}V_2O_{40}\cdot 22H_2O$)[13,15] and solid acidic salts (e.g., $CsHSO_4$ and CsH_2PO_4),[13,16] have been reported. However, these proton conductors indicate the decrease of the proton conductivity by the evaporation of hydrate water above 100 °C or high water solubility. Furthermore, many hydrate compounds with water molecules in molecular structure become impossible to maintain because of the long heating in the intermediate temperature region.[17] On the other hand, our mesoporous material is synthesized at the high temperature (>400 °C) and is stable at the intermediate temperature region. Additionally, by its high surface area, mesoporous material can maintain a lot of adsorption water in the pore structure. Especially, $TiO_2-P_2O_5$ CGMN has a high water-holding capacity by the chemisorption. As a result, CGMN material indicated the high proton conductivity with the thermal stability at intermediate temperature under 100% RH conditions.

In summary, we prepared $TiO_2-P_2O_5$ CGMN with water-holding capacity at an intermediate temperature region. This $TiO_2-P_2O_5$ CGMN showed the high proton conductivity of 2 $\times$ 10^{-2} S cm^{-1} at 160 °C under 100% RH. The CGMN may have a potential not only for the fuel cell electrolytes operated at intermediate temperature conditions but also for electrochemical devices, including electrochromic displays, chemical sensors, lithium rechargeable batteries, and others.

Supporting Information Available: Experimental procedure and Figure S1. This material is available free of charge via the Internet at http://pubs.acs.org.

References

(1) Li, Q.; He, R.; Jensen, J. O.; Bjerrum, N. J. *Chem. Mater.* **2003**, *15*, 4896.
(2) Hickner, M. A.; Ghassemi, H.; Kim, Y. S.; Einsla, B. R.; McGrath, J. E. *Chem. Rev.* **2004**, *104*, 4587.
(3) Sone, Y.; Ekdunge, P.; Simonsson, D. *J. Electrochem. Soc.* **1996**, *143*, 1254.
(4) Vichi, F. M.; Tejedor-Tejedor, M. I.; Anderson, M. A. *Chem. Mater.* **2000**, *12*, 1762.
(5) Halla, J. D.; Mamak, M.; Williams, D. E.; Ozin, G. A. *Adv. Funct. Mater.* **2003**, *13*, 133.
(6) Long, J. W.; Dunn, B.; Rolison, D. R.; Whilte, H. S. *Chem. Rev.* **2004**, *104*, 4463.
(7) Ozin, G. A. *Chem. Commun.* **2000**, 419.
(8) (a) Hogarth, W. H. J.; Costa, J. C. D.; Drennan, J.; Lu, G. Q. *J. Mater. Chem.* **2005**, *15*, 754. (b) Alberti, G.; Casciola, M.; Cavalaglio, S.; Vivani, R. *Solid State Ionics* **1999**, *125*, 91. (c) Rodríguez-Castellón, E.; Jiménez-Jiménez, J.; Jiménez-López, A.; Maireles-Torres, P.; Ramos-Barrado, J. R.; Jones, D. J.; Rozière, J. *Solid State Ionics* **1999**, *125*, 407. (d) Hamoudi, S.; Royer, S.; Kaliaguine, S. *Microporous Mesoporous Mater.* **2004**, *71*, 17. (e) Armento, P.; Casciola, M.; Pica, M.; Marmottini, F.; Palombari, R.; Ziarelli, F. *Solid State Ionics* **2004**, *166*, 19. (f) Mikhailenko, S.; Desplantier-Giscard, D.; Danumah, C.; Kaliaguine, S. *Microporous Mesoporous Mater.* **2002**, *52*, 29. (g) Matsuda, A.; Nono, Y.; Kanzaki, T.; Tadanaga, K.; Tatsumisago, M.; Minami, T. *Solid State Ionics* **2001**, *145*, 135.
(9) (a) Li, D.; Zhou, H. S.; Honma, I. *Nat. Mater.* **2004**, *3*, 65. (b) Zhou, H. S.; Li, D.; Hibino, M.; Honma, I. *Angew. Chem., Int. Ed.* **2005**, *44*, 797.
(10) Nogami, M.; Matsushita, H.; Goto, Y.; Kasuga, T. *Adv. Mater.* **2000**, *12*, 1370.
(11) (a) Honma, I.; Nakajima, H.; Nishikawa, O.; Sugimoto, T.; Nomura, S. *Solid State Ionics* **2003**, *162−163*, 237. (b). Nakajima, H.; Nomura, S.; Sugimoto, T.; Nishikawa, O.; Honma, I. *J. Electrochem. Soc.* **2002**, *149*, A953.
(12) (a) Yamada, M.; Honma, I. *Angew. Chem., Int. Ed.* **2004**, *43*, 3688. (b) Yamada, M.; Honma, I. *ChemPhysChem* **2004**, *5*, 724.
(13) Colomban, P.; Novak, A. *J. Mol. Struct.* **1988**, *177*, 277.
(14) Kreuer, K. D. *Chem. Mater.* **1996**, *8*, 610.
(15) Sang X. G.; Wu Q. Y. *Chem. Lett.* **2004**, *33*, 1518.
(16) (a) Boysen, D. A.; Uda, T.; Chisholm, C. R. I.; Haile, S. M. *Science* **2004**, *303*, 68. (b) Haile, S. M.; Boysen, D. A.; Chisholm, C. R. I.; Merle, R. B. *Nature* **2001**, *410*, 910. (c) Baranov, A. I.; Shuvalov, L. A.; Schagina, N. M. *JETP Lett.* **1982**, *36*, 459. (d) Baranov, A. I.; Khiznichenko, V. P.; Shuvalov, L. A. *Ferroelectrics* **1989**, *100*, 135.
(17) England, W. A.; Cross, M. G.; Hamnett, A.; Wiseman, P. J.; Goodenough, J. B. *Solid State Ionics* **1980**, *1*, 231.

JA052914X